A Compliant End-effector to Limit the Force in Tele-operated Tissue-Cutting

Santosh D.B. Bhargav, Shanthanu Chakravarthy, G. K. Ananthasuresh

Abstract

We present a compliant end-effector that helps in cutting soft tissues and sensing the cutting forces. The design of the end-effector is such that it has an upper threshold on cutting forces to facilitate safe handling of tissue during automated cutting. This is shown with nonlinear finite element analysis and experimental results obtained by cutting inhomogeneous phantom tissue. The cutting forces are estimated using a vision-based technique that uses deformation of the compliant end-effector. Furthermore, we demonstrate an immersive tele-operated tissue-cutting system together with a haptic device that gives real-time force feedback to the user.

Keywords: Compliant mechanisms, Tissue-cutting, Tele-operation, Haptics.

1 Introduction

Estimation of cutting forces is of importance in robot-assisted surgery and biomechanical studies [1]. Forces involved in cutting soft tissue are also important in developing virtual reality-based surgical training systems with haptic feedback [2, 3]. Cutting forces are estimated, in general, using material models for tissues [3-5] or measurements using off-the-shelf force sensors [6]. Material models for tissues do not fully capture inherent nonlinearities and inhomogeneity that exist in biological tissues. In reality-based techniques there is no direct way to passively (i.e. without control) limit the maximum cutting force that the tool exerts on the specimen as they are attached to stiff end-effectors. An end-effector that holds the scalpel overcomes this limitation and acts as a force sensor is the focus of this paper.

Our work encompasses design, development, and use of a compliant end-effector that can hold a scalpel and can also help measure the cutting force in a tele-operated system. The compliant mechanism used as the end-effector is easy to manufacture as it does not require much assembly; consequently, the procedure is cost-effective and is easy to implement in practice. Integrating any other, including commercial off-the-shelf (e.g. load-cell, polyvinylidene fluoride (PVDF) film-based) force sensors is not difficult at the macro scale but would become a challenge at the micro scale when one deals with isolated biological cells and tissue fragments. However, this paper describes only the macro-scale experiments on phantom tissues.

In the designed system, since a scalpel is attached to the compliant end-effector that is moved by a slave manipulator, the force applied by the scalpel is kept under check. Limiting the force is achieved inherently by the design of the compliant end-

Santosh D.B. Bhargav (Corresponding author)
Mechanical Engineering, Indian Institute of Science, Bangalore. Email: sbhargav@mecheng.iisc.ernet.in

Shanthanu Chakravarthy
Mechanical Engineering, Indian Institute of Science, Bangalore . Email: sc@mecheng.iisc.ernet.in

G. K. Ananthasuresh
Mechanical Engineering, Indian Institute of Science, Bangalore. Email: suresh@mecheng.iisc.ernet.in

effector. This feature of compliant end-effectors is beneficial in carefully removing the stiffer tumour from the surrounding soft tissue for pathological studies. Also, in tele-operated surgeries stiffer bone may need to be protected while handling the surrounding softer tissue.

Compliant mechanisms [7] transmit and transform motion/force using elastic deformation unlike jointed rigid-link assemblies. By using a Displacement-amplifying Compliant Mechanism (DaCM), we enhance the motion of the cutter (e.g., a scalpel) so that the amplified motion is visually measured, which is in turn correlated to the force exerted by the cutter on the tissue [8, 9]. Although the design of DaCMs is dependent on the inputs from the biological specimen, the working (including the force-sensing) is independent of the specimen. This is in contrast to other vision-based force-sensing techniques in which the deformation of the object is used for force-estimation. In order to meet 1000 Hz update rate of the haptic device, the force is estimated based on pre-computed force vs. displacement characteristic of the end-effector.

Figure (1) shows the tele-operation setup in which the user controls the master device (a haptic robot) to remotely operate a slave manipulator. The motion of the slave manipulator, mounted with the compliant end-effector, is used to cut the tissue.

The rest of the paper is organized as follows. The experimental setup is described in Section 2; the simulation, force-limiting feature, and calibration of force-sensing of the compliant mechanism are discussed in Section 3; results and discussion are presented in Section 4, and concluding remarks are given in Section 5.

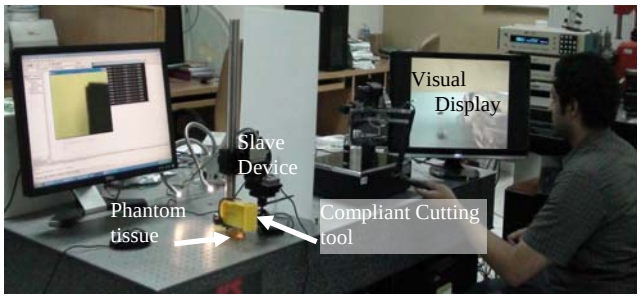

Figure 1: Tissue-cutting tele-operation setup.

2 The Setup

Our tele-operated soft tissue cutting setup consists of a 3-degree-of-freedom (dof) XYZ micro-positioner (MP-285, Sutter Inc.), two CMOS (complementary metal-oxide-semiconductor) cameras and a compliant mechanism-based polypropylene end-effector along with a scalpel. The close-up view of the setup is shown in Fig. (2). The force-sensing compliant mechanism and the camera mounted to facilitate image processing (camera1 at the output side of the compliant mechanism) are packaged in an acrylic casing. Here the compliant mechanism along with the acrylic casing containing the camera is referred as the compliant end-effector.

The compliant end-effector is moved by the XYZ positioner, which in turn is controlled by a remote user through a haptic device (PHANTOM Premium 1.5/6DOF HF, SensAble Technologies Inc.). The haptic device is connected to the master computer while the XYZ positioners are connected to a slave computer. The

two computers exchange data through local area network (LAN).

A remote user operates the stylus of the haptic device to provide motion to the cutter. The position of the stylus is fetched by the master computer from the haptic device and is sent to the remote slave computer connected through LAN. The slave computer commands the micro-positioner carrying the compliant end-effector to move and thereby cut the phantom tissue. The camera, mounted on to the compliant end-effector captures the image of the output point of the mechanism and passes it to the vision-based force-sensing algorithm on the slave computer, which in turn processes the image and sends the computed force to the master computer. The tissue-cutting force is scaled up to a suitable value and given to the user. The user is also given a visual feedback of the cutting operation with the help of another CMOS camera. Thus, the entire process of cutting takes place with the help of four concurrent computation threads: haptic thread, LAN communication thread, manipulator thread, and the vision-based force-sensing thread (see Fig. (3)). All these threads are implemented using Microsoft visual C++.

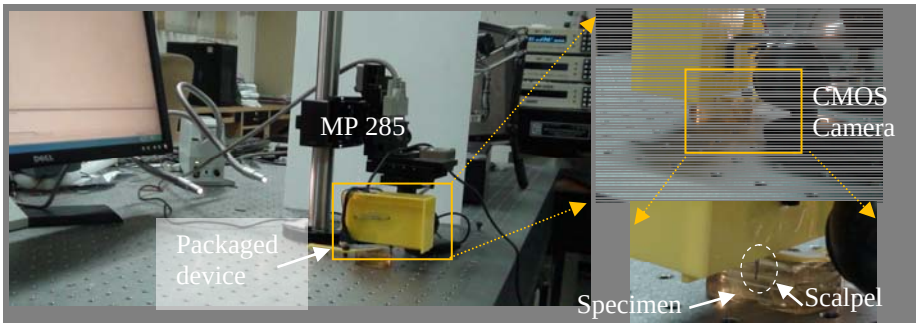

Figure 2: The slave manipulator cutting phantom tissue. The inserts show close-up views of the setup.

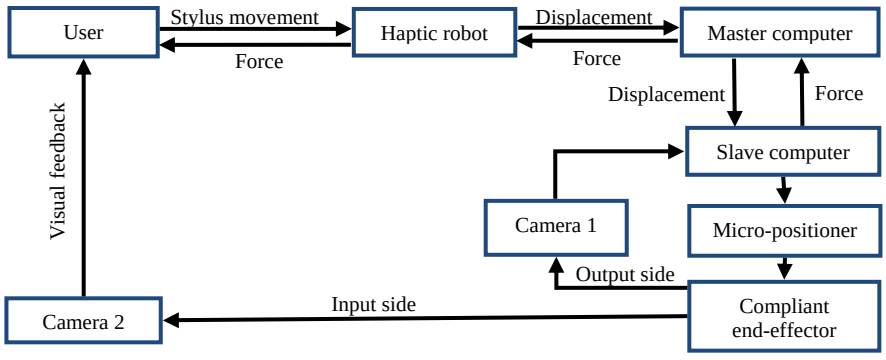

Figure 3: Flow of information in the tele-operated tissue-cutting setup.

3 Compliant End-effector

The compliant mechanism used in the end-effector was designed using the selection-map technique [10].The DaCM at its input is expected to have a deformation such that the scalpel attached to the compliant mechanism retracts as it encounters a stiffer

region. Among all the DaCMs listed in the database of the selection-map technique, the chosen DaCM has the aforementioned deformation characteristics. Furthermore, its overall size, the thickness, and the in-plane-widths of its slender beams were modified for a chosen material (polypropylene) and expected cutting force (up to 3 N). The design details are not presented here for brevity. The mechanism has an overall width of 70.7 mm and height of 47.6 mm. A 10 mm long surgical scalpel is attached rigidly to the mechanism. A drawing of the mechanism along with its dimensions and the fabricated polypropylene prototype are shown in Fig. (4). The end-effector was fabricated in-house using a Computer Numerical Control (CNC) milling machine.

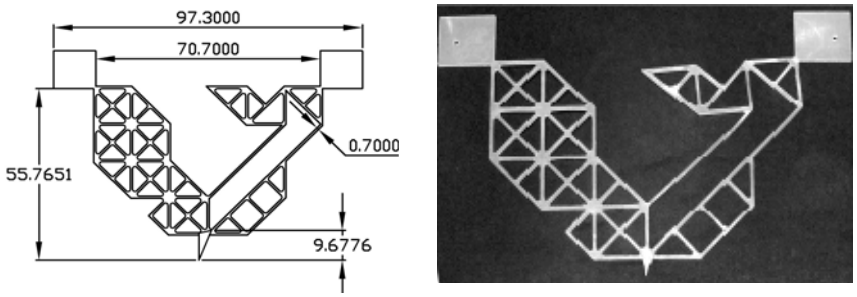

Figure 4: Geometric model and the fabricated mechanism serving as the compliant end-effector. All dimensions are in mm.

3.1 Limiting the cutting force

In this section, we explain how the cutting force is inherently limited by the compliant end-effector and how to estimate the maximum cutting force for a given depth of cut of the scalpel by referring to Fig. (5).

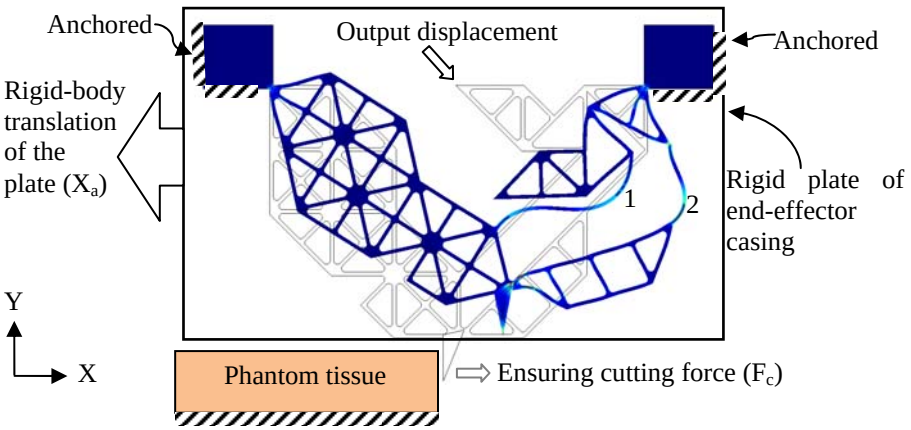

Figure 5: The end-effector, attached to a rigid plate, is moved to cut the specimen; some of the beams that buckle due to the force of cutting are pointed out.

In order to understand how the cutting force is limited, it is important to know how cutting is performed. The compliant mechanism is anchored on a rigid plate at two places as shown in Fig. (5). The rigid plate is part of the acrylic casing. The rigid

plate is translated to the left to enable the scalpel attached to the end-effector cut the phantom tissue. When the scalpel cuts the tissue, the cutting-force is experienced at the input of the end-effector. By virtue of this force, the beams present in the compliant end-effector undergo elastic deformation where some of them may also buckle under large forces. Deformation configuration of the mechanism, under a large load, is shown in Fig. (5). Beams marked 1 and 2 undergo local buckling that reduces the stiffness of the end-effector. As a result, the scalpel is automatically retracted away from the tissue. Although Fig. (5) shows the scalpel out of contact with the tissue in its deformed configuration, in reality it stops on the top edge of the tissue and begins to merely scratch or slide on it.

The finite element analysis of cutting the phantom tissue would involve: estimating the force applied by the scalpel blade on to the phantom tissue due to contact; accounting the fracture/cutting of the tissue; estimating the deformation of the mechanism. However, in order to simplify the analysis, the deformation configuration of the mechanism with a distributed load is used to mimic the traction boundary condition that the scalpel blade would undergo while it cuts the phantom tissue.

Large-deformation analysis of the mechanism using COMSOL MultiPhysics finite element software was carried out to estimate the limiting cutting force for any depth of the scalpel. Polypropylene was assumed to have a Young's modulus of 2 GPa and Poisson's ratio of 0.33. Simulation of cutting involves contact as well as fracture analyses. However, here a simplified method is adopted wherein the nonlinear force-displacement behaviour of the compliant end-effector is obtained a priori and is used later to estimate the cutting force and profile of the edge that is cut.

As shown in Fig. (6a) four points ($d_{1\text{-}4}$) are chosen on the scalpel and a force (F_c) is applied in increments to obtain force vs. displacement curves. The force is assumed to be the same at all four points of the scalpel. In this simulation, the scalpel is assumed to be free to move. Force in the Y-direction is not considered because it will be much less than the force in the cutting direction (i.e., X direction). The resulting X-component ($X_{e/a}$) and Y-component ($Y_{e/a}$) of the displacement of the scalpel relative to the rigid plate are shown in Figs. (6b-c). The curves in both figures show a significant decrease in the slope (i.e., stiffness) at about 1.5 N force. This is because the beams begin to locally buckle at this force. This is not catastrophic buckling because the beams are biased to bend right from the beginning.

It can be seen in Figs. (6b-c) that the X-displacements of the four points ($d_{1\text{-}4}$) are slightly different whereas Y-displacements are almost the same. Hence, a close-up view of a portion of the curves in Fig. (6c) is also shown. These curves are useful in estimating the maximum cutting force based on the depth of cut. For this, we use Fig. (6c) and read the cutting force for a particular value of $Y_{e/a}$ that is equal to the depth of cut. When $Y_{e/a}$ is more than the depth of cut, that point would have retracted away from the tissue and hence no more cutting occurs. Four vertical lines in Fig. (6c) correspond to the depths of cut shown in Fig. (6a) on the scalpel. For example, the maximum cutting force is 2.7 N for 6.89 mm depth of cut.

The curves in Figs. (6b-c) also help in predicting the cutting profile. To demonstrate this, we consider a tissue (see Fig. (7a)) with three regions of varying hardness. The starting portion of 15 mm needs a cutting force of 0.25 N, the next 12 mm needs 2 N, and the last 18 mm needs 1 N. These values were obtained based on prior experiments on phantom tissue specially prepared for experimental validation

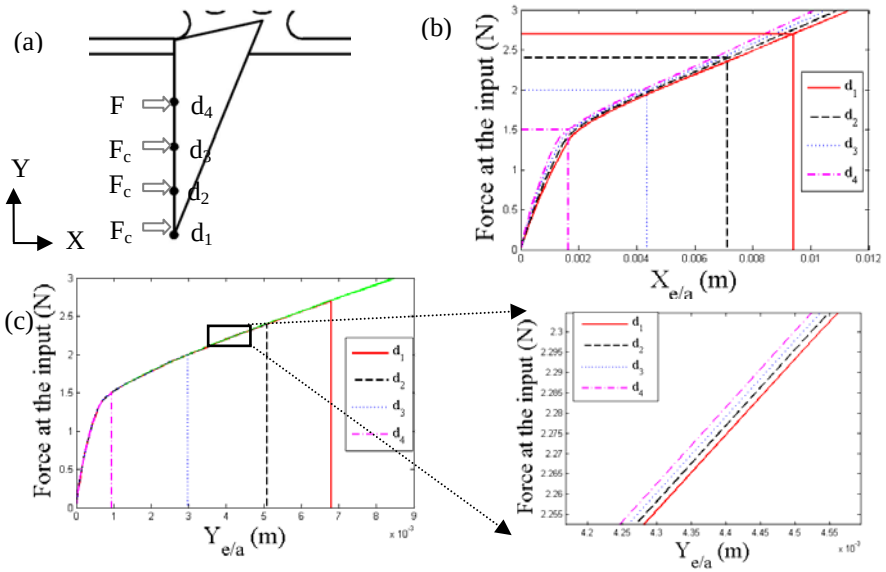

Figure 6: (a) The points on the scalpel chosen to apply the force (F_c). (b) X-displacement characteristic of the end-effector for the cutting-force (F_c) indicating the reaction in the overall stiffness of the mechanism in the cutting direction. (c) Lift-off of the scalpel for the cutting-force and the close-up view showing that the Y-displacement characteristic for the points $d_{1\text{-}4}$ is different (although very small).

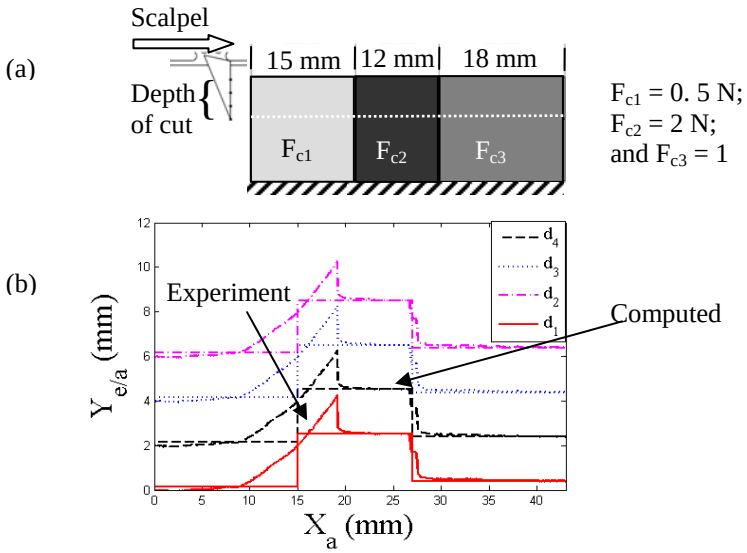

Figure 7: (a) A specimen to demonstrate lift-off-characteristic of the scalpel attached to the compliant end-effector. (b) Plot comparing the experimental and computed values of the Y-displacement of different points of the scalpel.

of the setup and technique. By reading off $X_{e/a}$ and $Y_{e/a}$ for different values of cutting forces using Figs. (6b-c), the locus of the cutting points can be determined. Hence,

the computed cutting profiles can be sketched as shown by curves with sharp corners in Fig. (7b). The smooth curves superimposed in this figure corresponding to the experimental results, as explained next.

For conducting the experiment, hybrid phantom tissue consisting of gelatin-based hydrogel that mimicks the soft tissue and polydimethylsiloxane (PDMS, Sylgaurd 184) that mimicks the stiffer region was prepared. The phantom tissue was cut in two separate steps due to the limited range (25 mm) of the micro-positioner. The specimen was initially cut through a distance of 25 mm through regions 1 and 2 of Fig. (7a). The remaining 18 mm part was cut after translating the micro-positioner and slicing off the initially cut portion. The points on the scalpel were imaged to measure their motion and track the cutting profile experimentally. The retraction of the scalpel can be seen in the smooth (i.e., experiment) curves in Fig. 7(b).

The behaviour of the experimentally obtained curves in Fig. (7b) is different from the computed ones. The first deviation is in the gradual rise of the profile as opposed to the sudden rise of the computed curves. This is because the portion of the hydrogel close to the PDMS part hardens and thus increases the required cutting force. The second deviation is the significant 'lift-off' in the experimental curve before it drops again. This is because of the inherent dynamics in the experiment despite the slow movement of the micro-positioner. When the scalpel encounters the hard portion, the scalpel lifts off the tissue in a jerky motion. The restoring force of the compliant end effector brings it back into contact with the tissue. From that point onwards, the scalpel slides or scratches on the top edge of the tissue.

The simulation described in this section assumed the value of cutting force. But the compliant end-effector has the additional feature of measuring the cutting force as described in the next section.

3.2 Force-sensing and calibration

When the compliant end-effector is moved to cut the tissue, the reaction force acts on the input side of the mechanism by virtue of which an amplified displacement is observed at the output point of the mechanism. The amplified displacement at the output of the mechanism is captured by a camera. A vision-based force-sensing routine employs an algorithm to detect the output edge from the binary image to measure the output displacement in terms of pixels. This displacement is used to find the reaction force from a pre-calibrated data of force vs. displacement curve of the compliant mechanism.

The displacement measured using vision-based technique has an uncertainty of ±1 pixel when image cross-correlation is not used. To account for this, a minimum of 5 pixel-displacement was considered for calibration. Hence, the compliant end-effector was made to move against the load-cell with in displacement steps of five pixels and the corresponding force detected by the load-cell was noted. Figure (8) is the output displacement vs. input force measured in the experiment. This data is used to compute the cutting force during real-time tele-operation. A 7th degree polynomial was used to fit the experimental data.

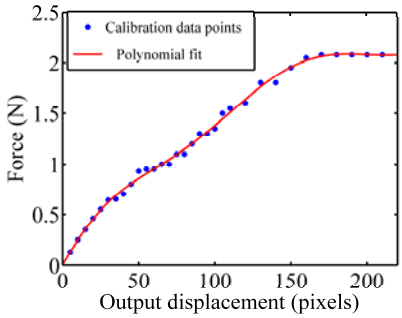

Figure 8: Input force vs. output displacement of the compliant cutter used for force-calibration.

4 Testing and Results

Phantom tissue with a stiff (PDMS) inclusion inside soft hyrdogel is shown in Fig. (9a). This was used to compare the compliant end-effector against a rigid end-effector. A load-cell carrying a scalpel at its end is used as a force-sensing rigid end-effector. Figure (9b) shows the measured forces in both the cases. It can be observed that the rigid end-effector (having an active upper-threshold of 5 N) cuts both the soft as well as the stiff region with the same depth of cut, while the compliant end-effector lifts off when it comes in contact with the stiffer region and maintains its threshold-force of about 2 N corresponding to a depth of cut of about 2.8 mm. As noted earlier, the depth of cut can be adjusted to change the threshold force.

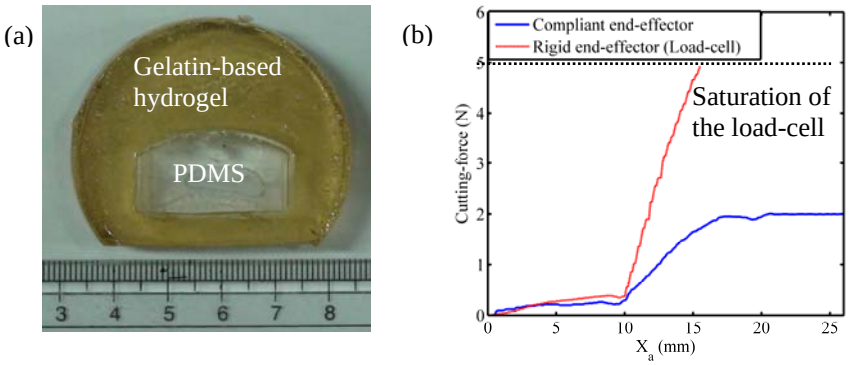

Figure 9: (a) Phantom tissue used in the experiments. (b) Plot comparing the forces measured by compliant and rigid end-effectors.

Experiments were also carried out to evaluate the immersive tele-operation system in which the user operates the stylus of the haptic robot to cut the phantom tissue consisting of regions of hydrogel and stiffer PDMS. Figure (10) is a plot of the measured force during one such remote tissue-cutting operation. When the scalpel comes in contact with the PDMS region of the phantom tissue it lifts off and while doing so, it drags the PDMS along with it. Just after the complete lift-off there is a

momentary loss of contact that makes the cutting force go down. After the momentary loss of contact the scalpel scratches the remaining part of the PDMS with minimal depth of cut. Thus, the PDMS region remains unharmed or minimally scratched while only the intended soft tissue (gelatin-based hydrogel) is cut.

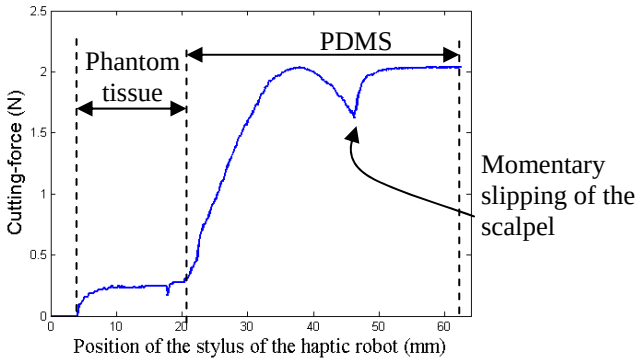

Figure 10: Measured force during tele-operated tissue-cutting operation.

5 Closure

In this paper, we described immersive tele-operated soft-tissue cutting procedure using a compliant end-effector. Compliant end-effector incorporates safety into tele-operation by retracting the scalpel beyond a threshold force for a chosen depth of cut, thereby minimizing the damage. A second use of the compliant end-effector is measuring the cutting force. A priori nonlinear FEA-based simulation and calibration with a load-cell were done. Simplified analysis in lieu of contact and fracture analyses was presented to help determine the depth of cut for desired upper threshold value for the cutting force. The procedure was experimentally validated and results were compared with those of a rigid end-effector attached to a load-cell. Tele-operation with a haptic robot was also presented to show that real-time operation is feasible. In both cases, the compliant end-effector did not cut the hard part as expected. The experiments were done on specially prepared inhomogeneous phantom tissue consisting of soft hydrogel and stiffer PDMS. To fully demonstrate the capability and applicability of this device, tissue-cutting with compliant end-effectors has to be tested with real tissues. Testing and evaluation of the system under actual surgical situation or dissection is the future course of this work.

Acknowledgements

We would like to thank G. Ramu, A. Ravi Kumar, M. P. Sajeesh Kumar and M. Suma for their help in fabricating the prototypes and arranging the experimental set-up. Special thanks to A.N. Reddy for his valuable inputs. Financial support from the Swarnajayanthi Fellowship of the Department of Science and Technology (DST) of the Government of India is also gratefully acknowledged.

References

[1] S. Greenish, V. Hayward, V. Chial, A. Okamura, and T. Steffen, "Measurement, analysis, and display of haptic signals during surgical cutting," Presence, vol. 11, pp. 626-51, 2002.

[2] O. A. J. van der Meijden, M. P. Schijven, "The value of haptic feedback in conventional and robot-assisted minimal invasive surgery and virtual reality training: a current review," Surgical Endoscopy, pp. 1180–1190, 2009.

[3] C. C. Hu J, Tardella N, Pratt J, English J, "Effectiveness of haptic feedback in open surgery simulation and training systems," Studies in Health Technology and Informatics, 2006.

[4] A. M. Okamura, R. J. Webster, III, J. T. Nolin, K. W. Johnson, and H. Jafry, "The haptic scissors: cutting in virtual environments," presented at IEEE International Conference on Robotics and Automation. IEEE ICRA 2003 Conference Proceedings, 14-19 Sept. 2003, Piscataway, NJ, USA, 2003.

[5] C. Simone and A. M. Okamura, "Modeling of needle insertion forces for robot-assisted percutaneous therapy," presented at Proceedings 2002 IEEE International Conference on Robotics and Automation, 11-15 May 2002, Piscataway, NJ, USA, 2002.

[6] T. Chanthasopeephan, J. P. Desai, and A. C. W. Lau, "Deformation resistance in soft tissue-cutting: a parametric study," presented at Proceedings. 12th International Symposium on Haptic Interfaces for Virtual Environment and Teleoperator Systems, 27-28 March 2004, Los Alamitos, CA, USA, 2004.

[7] L. L. Howell, Compliant Mechanisms. New York: Wiley, 2001.

[8] X. Wang, G. K. Ananthasuresh, and J. P. Ostrowski, "Vision-based sensing of forces in elastic objects," Sensors and Actuators A (Physical), Vol. A94, pp. 142-56, 2001.

[9] A. N. Reddy, N. Maheshwari, D. K. Sahu, and G. K. Ananthasuresh, "Miniature Compliant Grippers With Vision-Based Force-sensing,", IEEE Transactions on Robotics, vol. 26, pp. 867-877, 2010.

[10] S. Hegde and G. K. Ananthasuresh, "Design of Single-input-single-output Compliant Mechanisms for Practical Applications Using Selection Maps," Journal of Mechanical Design, vol. 132, pp. 081007 (8 pp.), 2010.